Adsorption 10: 99–109, 2004

Adsorption Kinetics and Dynamic Behavior of a Carbon Monolith

F. BRANDANI, A. ROUSE*, S. BRANDANI* AND D.M. RUTHVEN†
Department of Chemical Engineering, University of Maine, Orono, ME 04469-5737, USA

Received February 14, 2003; Revised December 22, 2003; Accepted January 5, 2004

Abstract. The zero length column (ZLC) method has been applied to study the adsorption and diffusion of CO_2 in a carbon monolith adsorbent. ZLC desorption curves, measured over a wide range of flow rates, are shown to be very well accounted for assuming a linear equilibrium isotherm with the kinetics controlled by diffusion into a parallel sided slab. The data, at all flow rates, are characterized by a single pair of parameters (K and D_s). Diffusivities for a He carrier are about double those for a N_2 carrier reflecting both the difference in molecular diffusivities and some contribution from Knudsen diffusion. Breakthrough curves for CO_2-He and CO_2-N_2 were also measured for columns packed with the monolith adsorbent. Both the equilibrium and diffusion parameters derived from analysis of the breakthrough curves in accordance with the Golay/Spangler models are consistent with the values derived from the ZLC measurements. Dispersion in the monoliths is shown to be controlled by mass transfer resistance rather than axial mixing.

Keywords: ZLC, CO_2, carbon monolith

Introduction

Monolithic adsorbers have been shown to offer important practical advantages over traditional packed adsorbent columns for applications such as rapid cycle pressure swing adsorption, VOC removal, desiccant cooling and other processes where pressure drop has a significant economic impact (Ruthven, 2000; Ruthven and Thaeron, 1996). Efficient performance as a mass transfer device requires that both the wall thickness and the cell dimensions of the monolith should be small and this requirement presents an important manufacturing challenge. However, this challenge has now been largely met, at least for carbon based monoliths, and monolithic carbon adsorbents with sufficiently small wall thickness and channel dimensions to be of interest for such applications are now available commercially (Park et al., 2001). This investigation, aimed at characterizing the adsorption kinetics and equilibria for CO_2, was undertaken as part of a detailed experimental and theoretical study of the performance of a rapid cycle dual piston pressure swing adsorption system using a monolithic carbon adsorbent. The measurements were carried out by both zero length column (ZLC) and breakthrough experiments with generally consistent results.

Details of Monoliths

Two carbon based monoliths, formed by extrusion of an activated carbon adsorbent together with a ceramic material to improve the physical strength were kindly provided by MeadWestvaco Corporation. Details of the dimensions are given in Fig. 1. The larger monolith was provided in cylindrical sections of 10 cm in length and 2.9 cm diameter. Five of these sections were connected in series to form an experimental column of effective length approximately 50 cm. The smaller monolith was available as rectangular sections $6 \times 4.7 \times 1$ cm. 45 cylindrical sections of diameter 1.56 cm were cut from

*Department of Chemical Engineering, University College London, Torrington Place, London WC1E7JE. Dr. Brandani is holder of the Royal Society/Wolfson Research Merit Prize.
†To whom correspondence should be addressed.

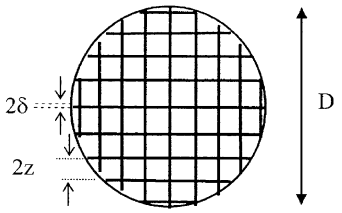

Larger monolith

D	2.9cm
2z	0.136cm
δ	0.014cm
L	50cm
ε	0.69

Smaller monolith

D	1.56cm
2z	0.09cm
δ	0.00825cm
L	45cm
ε	0.71

where $\varepsilon = \frac{z^2}{(\delta + z)^2}$

Figure 1. Schematic diagram showing form and dimensions of monoliths.

this base material and packed into a cylindrical tube of this diameter and length 45 cm to form a second column.

ZLC Measurements

Full details of the ZLC technique have been given elsewhere (Brandani et al., 2002; Eic and Ruthven, 1989; Ruthven and Brandani, 2000). In essence a small sample of adsorbent is pre-equilibrated with sorbate and then purged with an inert gas stream, at constant flow rate, monitoring continuously the concentration of sorbate in the effluent stream. At low flow rates the sample is essentially at equilibrium with the purge gas and the desorption curve yields the equilibrium isotherm while, at higher flow rates, the sorbate concentration in the effluent depends on the rate of diffusion out of the adsorbent. Under these conditions the response curve yields the diffusional time constant. ZLC measurements carried out over a wide range of flow rates thus provide a simple and convenient way to obtain both kinetic and equilibrium data.

In the low flow rate (equilibrium controlled) regime the ZLC response curve for a system with a linear isotherm is given by:

$$\frac{c}{c_o} = \exp\left[\frac{-Ft}{V_g + KV_s}\right] \tag{1}$$

The term $(V_g + KV_s)$ represents the hold up in the gas volume of the cell (V_g) plus the hold up in the adsorbed phase (KV_s). When adsorption is relatively weak the correction for hold up in the gas phase becomes significant. The value of V_g is conveniently determined from the blank response for the cell with no adsorbent present.

Under conditions of kinetic control the ZLC response for a parallel sided slab of adsorbent is given by:

$$\frac{c}{c_o} = \sum \frac{2Le^{-\beta^2\tau}}{(1+\gamma)\beta^2 + L + (L - \gamma\beta^2)^2} \tag{2}$$

where β is given by the roots of the equation

$$L - \gamma\beta^2 - \beta\tan\beta = 0 \tag{3}$$

and $\tau = D_s t/\ell^2, \gamma = V_g/KV_s, L = F\ell^2/KV_sD_s$. The derivation of Eq. (2) is given in the Appendix. Note that when γ is small (negligible gas phase hold up) the solution reduces to the simpler form given previously (Eic and Ruthven, 1989; Ruthven and Brandani, 2000).

In the present system the effluent gas composition was monitored using an on-line quadrupole mass spectrometer but any sufficiently sensitive detector can be used. A relatively large amount of adsorbent (7.6 mg) was used in the column to compensate for the low capacity.

Dead Volume Measurements

Figure 2 shows the blank response at several flow rates with both He and N_2 as carrier. It is evident that the

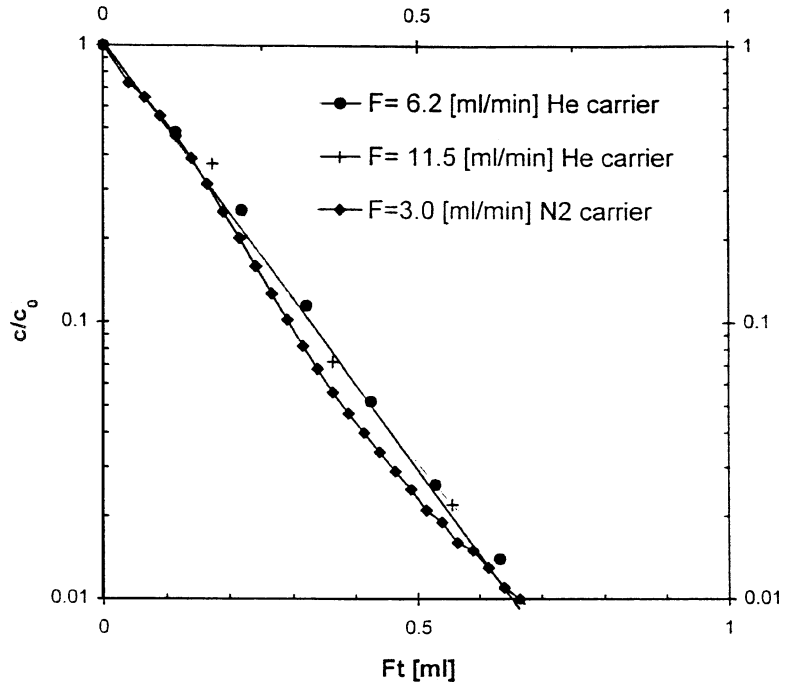

Figure 2. Blank ZLC response curves for CO_2 at 303 K.

response can be represented reasonably well by Eq. (1) (with $V_s = 0$). The dead volume calculated from the slope is approximately 0.14 ml.

Kinetic and Equilibrium Measurements

ZLC measurements for CO_2 in a small piece of the smaller monolith were carried out at 303 K over a wide range of flow rates, with either N_2 or He as the carrier/purge gas. Representative response curves are shown in Fig. 3. The response curves were fitted to Eqs. (2) and (3) (with $V_g = 0.14$ ml) using a least squares criterion to determine the best fit values of the two parameters (KV_s and D_s/ℓ^2) for each data set. This procedure has been shown to provide a more accurate method of parameter evaluation compared with the more traditional approach of fitting each response curve individually (Brandani et al., 1995). The values of these parameters are summarized in Table 1 and the theoretical curves, back calculated from Eq. (2) with the given parameter values, are shown in Fig. 3. It is clear that the theoretical curves, with a single pair of parameters, provide an excellent representation of the experimental response, for both the He and N_2 systems, over the entire range of flow rates. Furthermore, the response curves at the lowest flow rate conform to a simple exponential decay, in conformity with Eq. (1), the solution for equilibrium control. It is clear that the model of a linear equilibrium system in which the kinetics of desorption are controlled by diffusion out of a parallel sided slab provides an excellent representation of the observed behavior.

Table 1. Summary of parameters derived from ZLC measurements (smaller monolith at 303 K).

	He carrier	N_2 carrier
Dead volume V_g (ml)	0.14	
$KV_s + V_g$ (ml)	0.38	0.32
K	42.1	31.6
D_s/ℓ^2 (s^{-1})	0.92	0.48
D_s ($cm^2 \cdot s^{-1}$)	6.3×10^{-5}	3.3×10^{-5}

Sample wt = 7.6 mg, Density = 1.33 g/ml, $V_s = 5.7 \times 10^{-3}$ ml, $\ell = 0.0083$ cm.

Breakthrough Measurements

A series of breakthrough experiments was carried out with the columns formed by connecting sections of the

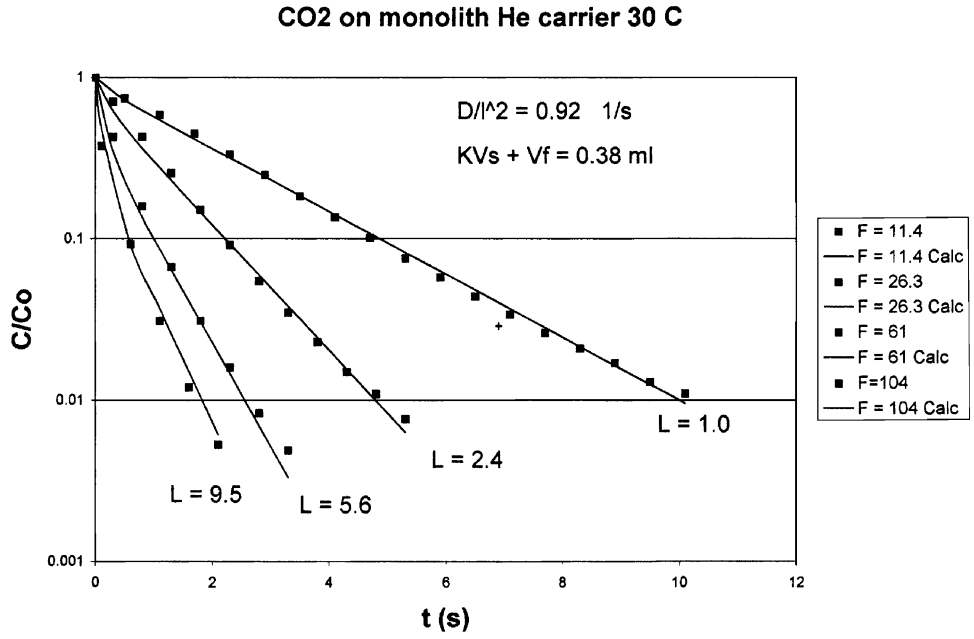

(a)

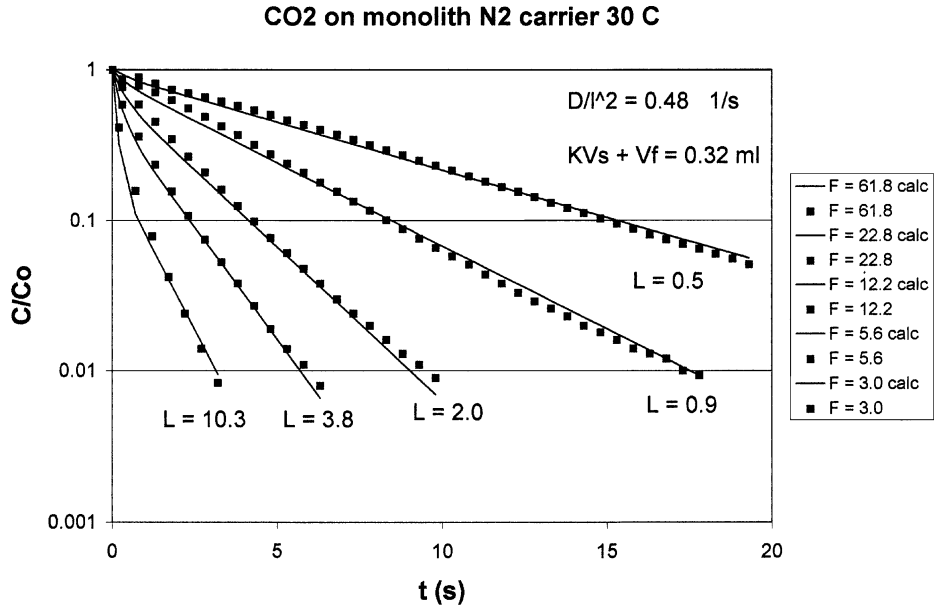

(b)

Figure 3. ZLC response curves for CO_2 at 303 K. (a) He and (b) N_2 purge gas. Initial CO_2 partial pressure = 23 Torr. Purge flow rates (F) are in ml/min.

monoliths in series. Details of the column dimensions are given in Table 2. The breakthrough curves were measured, at several different flow rates with a feed stream containing about 1% CO_2 in a carrier of either N_2 or He. Both the adsorption and desorption curves were measured. At constant flow rate the adsorption response was always somewhat sharper than the desorption response suggesting that, even at this low concentration level, the equilibrium isotherm is of slightly favorable form. The symmetry between adsorption and

Table 2. Summary of column dimensions and parameters derived from breakthrough measurements at 296 K.

	Smaller monolith	Larger monolith	
Cross sectional area (cm^2)	1.91	6.6	
Column length L (cm)	45	50	
Voidage ε	0.71	0.69	
Internal cell dimension 2z (cm)	0.09	0.136	
Wall thickness 2w (cm)	0.0165	0.028	
Carrier	N_2	N_2	He
Slope of μ vs. 1/F (ml)	1153	4319	5333
Slope of H vs. F ($s \cdot cm^{-2}$)	0.12	0.247	0.095
K	44.4	39.7	49.5
D_s($cm^2 \cdot s^{-1}$)	1.93×10^{-5}	7.4×10^{-6}	3.55×10^{-5}
Molecular diffusivities (D_g) at 296 K	CO_2-He, 0.63 $cm^2 \cdot s^{-1}$; CO_2-N_2, 0.17 $cm^2 \cdot s^{-1}$		

desorption breakthrough curves has been shown to be extremely sensitive to minor deviations from linearity in the equilibrium isotherm. It is worth pointing out that this asymmetry cannot be explained by non-isothermality since, for a linear system, any temperature excursions should affect adsorption and desorption equally, leading to a broadening of the response but not to a divergence between the adsorption and desorption curves. The equivalent linear response was obtained by averaging the adsorption and desorption breakthrough curves (c/c_o vs. t and $1 - c/c_o$ vs. t) as shown in Fig. 4(b). Since the detector calibration is linear the dimensionless response curves are easily calculated from the detector signal (Fig. 4(a)). Kinetic and equilibrium parameters were then derived from these averaged curves by the method of moments.

The first and second moments were calculated directly from the breakthrough curves by integration (Ammons et al., 1977; Kärger and Ruthven, 1992).

$$\text{1st Moment:} \quad \mu = \int_o^\infty (1 - c/c_o)\, dt \tag{4}$$

$$\text{2nd Moment:} \quad \sigma^2 = 2\int_o^\infty (1 - c/c_o)t \cdot dt - \mu^2 \tag{5}$$

The first moment is related directly to the dimensionless Henry constant (K):

$$\mu = \frac{V}{F}[\varepsilon + (1 - \varepsilon)K] \tag{6}$$

Values of K, given in Table 2, were calculated from the slopes of the (linear) plots of μ vs. 1/F, shown in Fig. 5.

The expressions for the second moment of the response for a circular tube and a parallel sided duct, coated with an adsorbent layer were derived many years ago by Golay (1958). More recently the corresponding expression for a rectangular duct was derived by Spangler (1998, 2001). Since the cells of the present monoliths are square Spangler's expression is directly applicable to the present systems provided that the thickness of the adsorbent layer is replaced by the half thickness of the monolith walls. This yields:

$$\frac{H}{2} = \frac{\sigma^2}{2\mu^2} \cdot L = \frac{D_g}{\bar{v}} + \left[\frac{70}{96} \cdot \frac{z^2}{D_g} + \frac{1}{6}\frac{wz}{KD_s}\right]\bar{v} \tag{7}$$

which is, except for the coefficient 70/96, the same as the Golay expression for a circular duct of radius z (Golay, 1958). Except at very low flow rates the term $D_g/\bar{v}$ is negligible so Eq. (7) predicts a linear increase of HETP with flow rate. HETP values, calculated from the first and second moments of the averaged step response are shown plotted against flow rate in Fig. 6. The values of KD_s and D_s, calculated from the slopes of these plots, are given in Table 2.

Comparison of Kinetic and Equilibrium Parameters

Exact correspondence between the parameters derived from the ZLC and breakthrough measurements cannot be expected since the former were carried out at 30°C and the latter at approximately 23°C. The isosteric heat of adsorption for CO_2 on activated carbon is approximately 23 kJ/mole which yields a value of 1.24 for the ratio of K values at 23°C and 30°C. For the smaller monolith, with N_2 as carrier, the corrected ZLC K value at 296 K is therefore 39.2, which agrees well with the value of 39.7 from the breakthrough measurements.

Both the ZLC measurements (smaller monolith) and the breakthrough measurements (larger monolith) show that the K value for CO_2-He is larger by about 25–30% than the value for CO_2-N_2. This is consistent with competitive adsorption of N_2 which, although

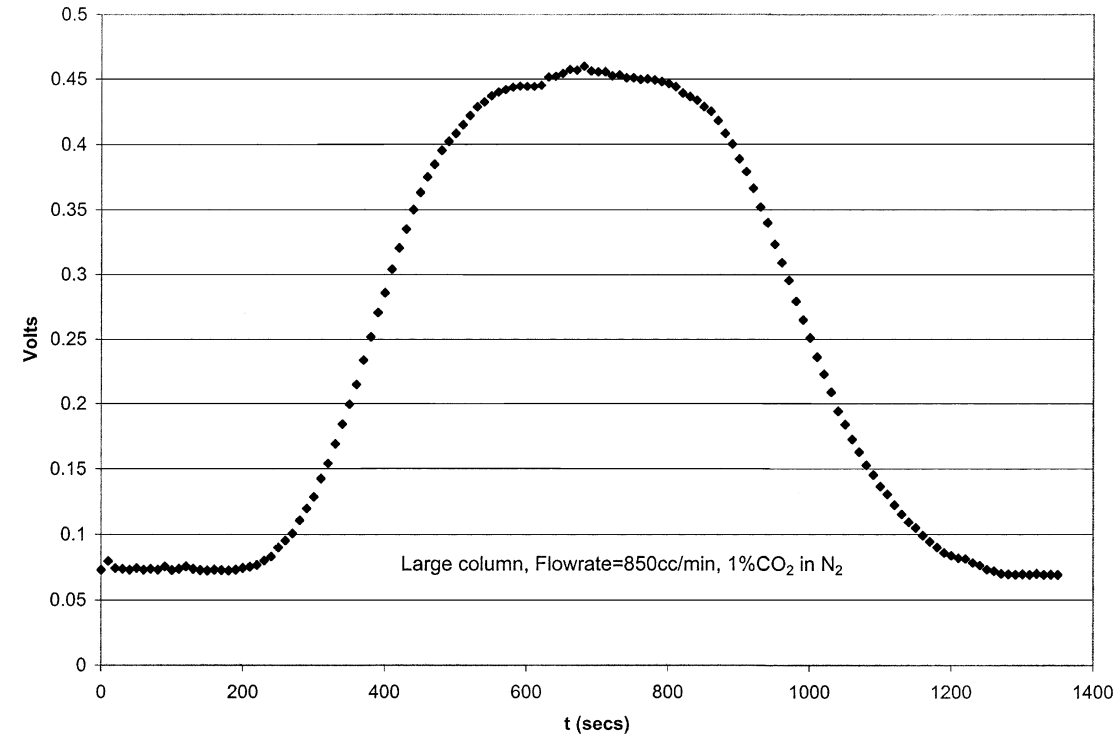

(a)

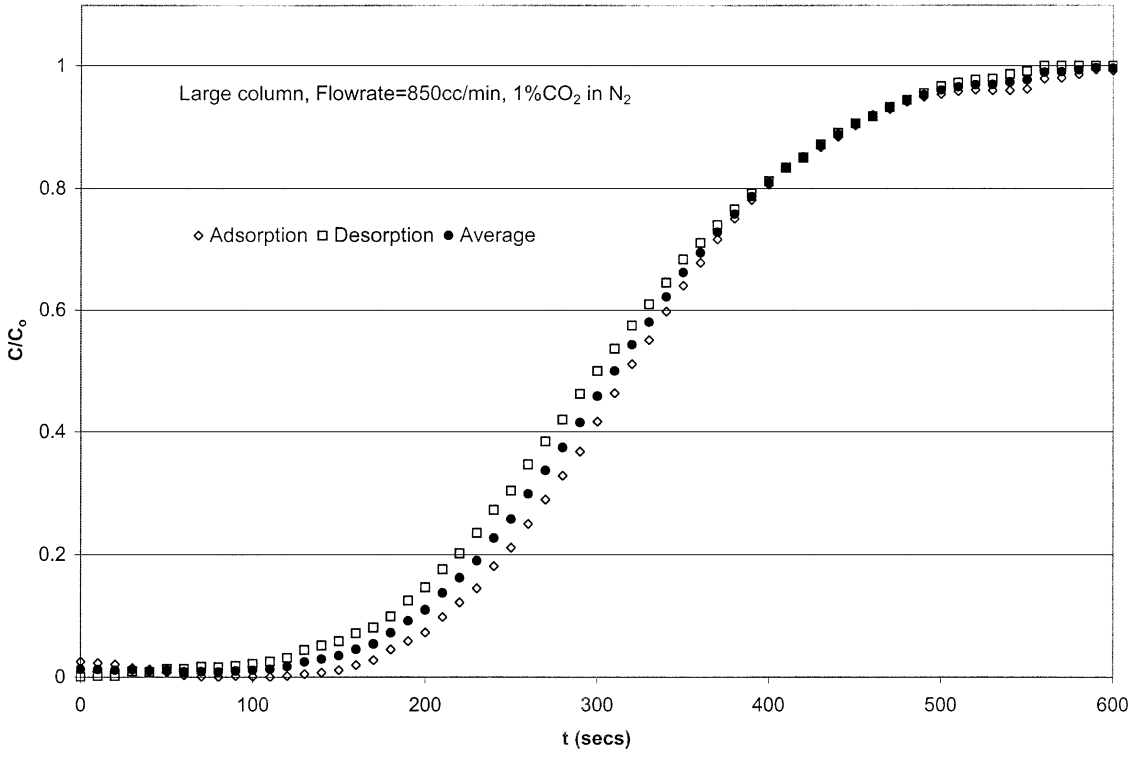

(b)

Figure 4. Representative breakthrough curves showing (a) adsorption and desorption curves and (b) the average (linear) curve.

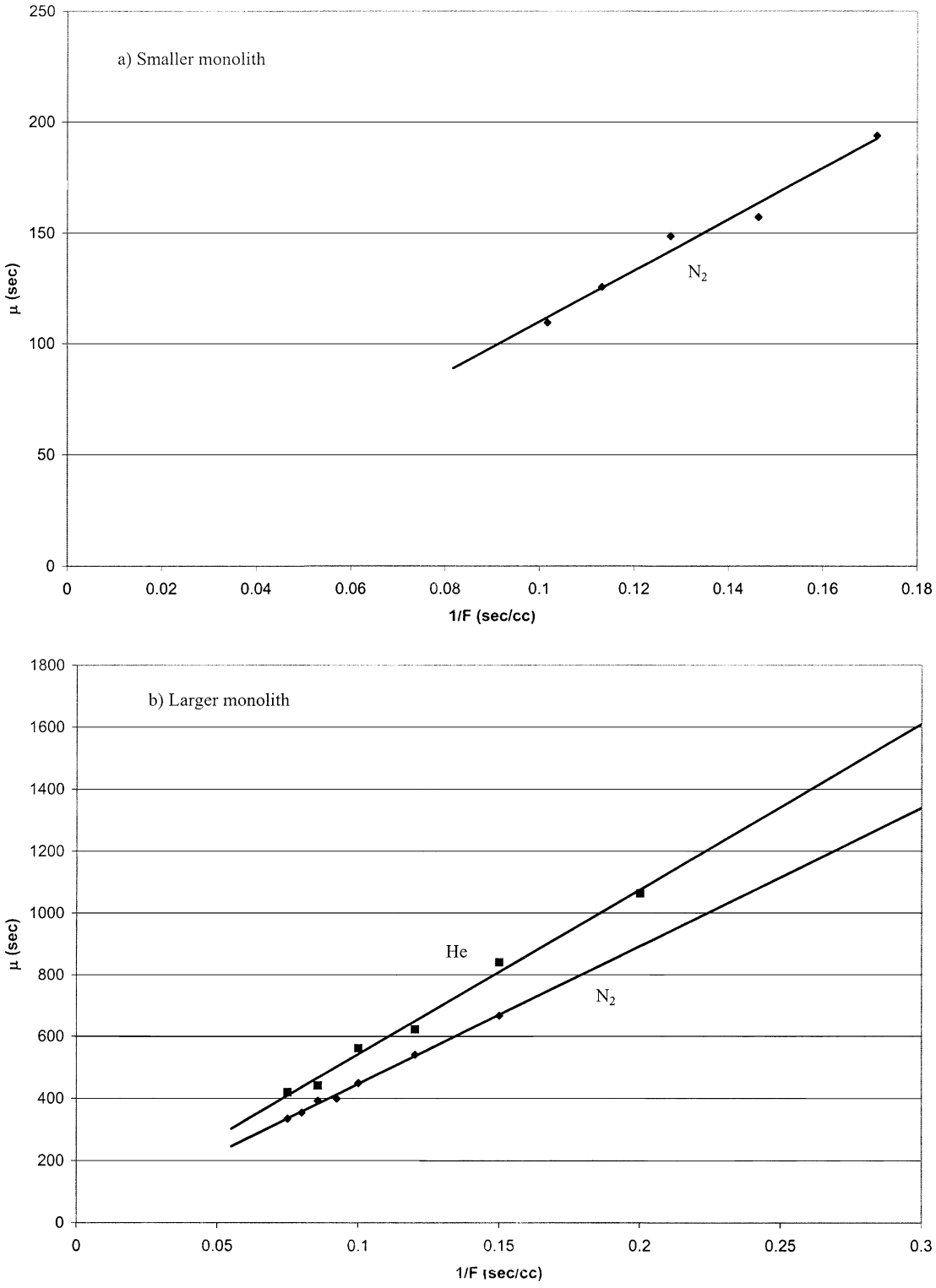

Figure 5. Variation of 1st moment with reciprocal flow rate for (a) small monolith and (b) large monolith.

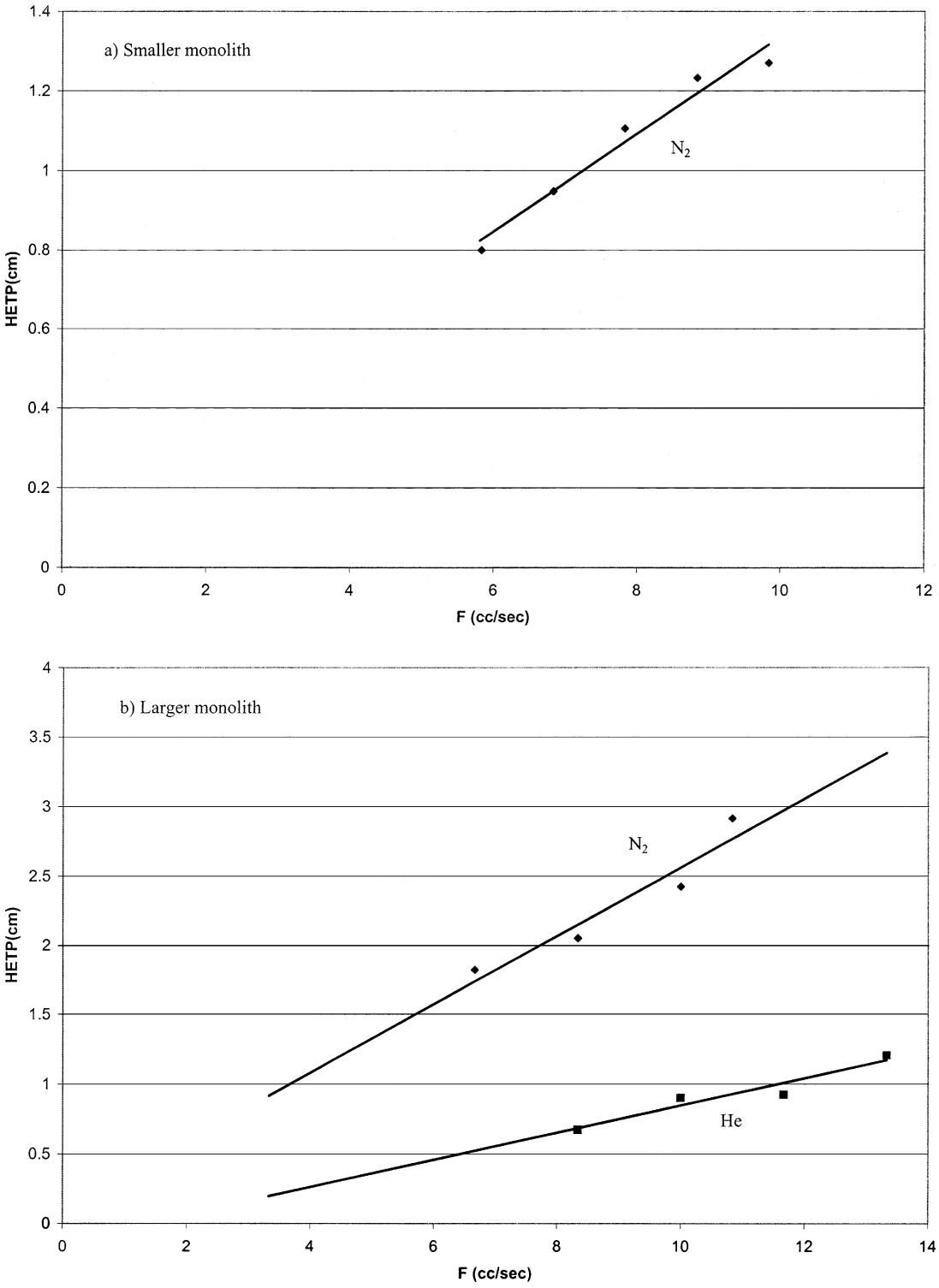

Figure 6. Variation of HETP with flow rate for CO_2 at 298 K with (a) small monolith and (b) larger monolith.

weakly adsorbed in comparison with CO_2 is present at a much higher partial pressure. The K values for CO_2-N_2 determined for the small and large monoliths from the breakthrough measurements agree within about 10%.

The agreement between the diffusivity values determined by ZLC and from the breakthrough curves is less satisfactory. For the smaller monolith for CO_2-N_2 the ZLC and breakthrough diffusivity values (3.3×10^{-5} and 1.93×10^{-5} $cm^2 \cdot s^{-1}$ respectively) differ by a factor of about 1.7. Both the ZLC measurements (smaller monolith) and the breakthrough measurements for the larger monolith show that the diffusivity for CO_2-He is substantially larger than that for CO_2-N_2. Such a difference is to be expected if transport within the pores is controlled mainly by Knudsen diffusion with some contribution from molecular diffusion. Comparison of the CO_2-N_2 data for the larger and smaller monoliths (derived from the breakthrough data) suggests that diffusion in the larger monolith is somewhat slower but since ZLC measurements were made only for the smaller monolith this conclusion could not be confirmed from the ZLC data.

The calculation of solid phase diffusivities from experimental breakthrough curves is subject to considerable error as a result of both the errors involved in the calculation of the second moments and the errors associated with the subtraction of the axial diffusion and Golay dispersion terms in Eq. (7). Nevertheless, with the exception of the breakthrough data for CO_2-N_2 in the larger monolith, the diffusivity values derived from the ZLC and breakthrough measurements appear to be reasonably consistent. For CO_2-N_2 in the smaller monolith, the ZLC and breakthrough diffusivities agree within a factor of about 1.7 (3.3×10^{-5} and 1.93×10^{-5} $cm^2 \cdot s^{-1}$). Some of this difference can be attributed to the difference in temperature between the ZLC (30°C) and the breakthrough experiments (23°).

The ZLC data (for the smaller monolith), which should be reliable, suggest that the pore diffusivity for CO_2-He is greater than that for CO_2-N_2 by a factor of about two. A similar difference is seen between the breakthrough diffusivities for CO_2-He in the larger monolith and CO_2-N_2 in the smaller monolith. Since the equilibrium constants for the smaller and larger monoliths are consistent it may be reasonable to assume that the pore size, and therefore the pore diffusivities, are also similar. A difference in diffusivity of this magnitude is to be expected if transport within the pores occurs by a combination of the Knudsen and molecular diffusion mechanisms since the molecular diffusivity for CO_2-He is substantially larger than for CO_2-N_2. However, on the basis of these comparisons, the breakthrough diffusivity for CO_2-N_2 in the larger monolith appears to be erroneously small by a factor of about two. This might suggest additional dispersion in the larger monolith arising from non-ideality of the monolith structure since the effects of axial mixing and mass transfer resistance in spreading the breakthrough response are very similar.

Conclusions

The following conclusions can be drawn from this study:

1. The ZLC response curves, which were measured over a wide range of flow rates, show clearly the transition from equilibrium control at low purge rates to kinetic control at high flow rates. Over the entire range the simple model (Eq. (2)) with constant values of the two parameters D/ℓ^2 and K, provides an excellent representation of the dynamic behavior.
2. The Spangler expression (Eq. (7)) provides a good representation of the breakthrough curves and yields kinetic and equilibrium parameters which are approximately consistent with the ZLC values.
3. The pore diffusivities for CO_2-He are approximately double the values for CO_2-N_2 suggesting that diffusion occurs by a combination of the molecular and Knudsen mechanisms. The possibility of some additional contribution from micropore resistance cannot be excluded.

Appendix

ZLC Response for Parallel Sided Slab with Significant Gas Phase Hold-Up

$$V_s \frac{d\bar{q}}{dt} + V_g \frac{dc}{dt} + Fc = 0$$

$$\frac{\partial q}{\partial t} = 2A D_s \frac{\partial q}{\partial x}\bigg|_{x=l}$$

Boundary conditions:

$$\left.\frac{\partial q}{\partial x}\right|_{x=0} = 0, \quad q|_{x=l} = Kc$$
$$V_s \frac{d\bar{q}}{dt} = 2A_s D_s \left.\frac{\partial q}{\partial x}\right|_{x=l}$$

Dimensionless variables:

$$\xi = x/l, \quad \tau = D_s t/l^2, \quad Q = q/q_o = q/Kc_o,$$
$$C = c/c_o, \quad \gamma = V_g/KV_s, \quad L = Fl^2/KV_sD_s$$
$$\left.\frac{\partial Q}{\partial \xi}\right|_1 + \gamma \frac{dC}{d\tau} + LC = 0$$
$$\frac{\partial Q}{\partial \tau} = \frac{\partial^2 Q}{\partial \xi^2}, \quad \left.\frac{\partial Q}{\partial \xi}\right|_o = 0, \quad Q_1 = C$$

Transforming to the Laplace domain yields:

$$\left.\frac{d\tilde{Q}}{d\xi}\right|_1 + \gamma(s\tilde{c} - 1) + L\tilde{c} = 0$$
$$s\tilde{Q} - 1 = \frac{d^2\tilde{Q}}{d\xi^2}$$

The Laplace domain solution is:

$$\tilde{C} = \frac{1}{s}\left[\frac{\sqrt{s}\tan h\sqrt{s} + \gamma s}{\sqrt{s}\tan h\sqrt{s} + \gamma s + L}\right]$$

Inversion by the method of residues yields for the time domain solution:

$$\frac{c}{c_o} = \sum_{n=1}^{\infty} \frac{2Le^{-\beta^2\tau}}{L + (1+\gamma)\beta^2 + (L - \gamma\beta^2)^2}$$

where β is given by the roots of the equation

$$\beta \tan\beta = L - \gamma\beta^2$$

Notation

A_s	External area
c	Sorbate concentration in gas phase
c_o	Initial (steady) value of c (ZLC experiment) or feed concentration for $t > 0$ (breakthrough experiment)
D_g	Molecular diffusivity (gas phase)
D_s	Pore diffusivity in solid (defined with respect to adsorbed phase concentration gradient)
F	Purge flow rate
H	Height equivalent to a theoretical plate (HETP)
K	Dimensionless equilibrium constant
ℓ	Half thickness of adsorbent
L	Parameter in Eqs. (2) and (3) defined by $L = F\ell^2/KV_sD_s$. Column length (in Eq. (7))
q	Adsorbed phase concentration (local)
$\bar{q}$	Average value of q
q_o	Value of q at equilibrium with c_o
t	Time
$\bar{v}$	Interstitial gas velocity
V	Column volume
V_g	Dead volume (in ZLC system)
V_s	Solid volume (in ZLC experiment)
w	Half thickness of monolith wall
x	Distance measured from center of slab
z	Half of internal cell dimension
μ	Mean retention time
ε	Voidage of monolith
σ^2	Second moment of chromatographic response
β, γ	Parameters in Eq. (2)

Acknowledgments

We are grateful to Dr. John Glomb, formerly of Mead-Westvaco Corporation for provision of the carbon monoliths. Financial support from the Engineering and Physical Sciences Research Council (UK) grant GR/R22087/01 and from the Leverhulme Prize is also gratefully acknowledged.

References

Ammons, R.D., N.A. Dougherty, and J.M. Smith, *Ind. Eng. Chem. Fund.*, **16**, 363 (1977).

Brandani, F., S. Brandani, C.G. Coe, and D.M. Ruthven, "Measurement of Henry Constants and Equilibrium Isotherms by the ZLC Technique," in *Fundamentals of Adsorption 7*, K. Kaneko, H.

Kanoh, and Y. Hanzawa (Eds.), pp. 21–28, International Adsorption Society, I.K. International, Chiba Japan 2002.

Brandani, S., D.M. Ruthven, and J. Kärger, "Concentration Dependence of Self-Diffusivity of Methanol in NaX Zeolite Crystals," *Zeolites*, **15**, 494–495 (1995).

Eic, M. and D.M. Ruthven, "Intracrystalline Diffusion of Linear Paraffins and Benzene in Silicalite Studied by ZLC," in *Zeolites Facts, Figures, Future*, P.A. Jacobs and R.A. van Santen (Eds.), pp. 897–905, Elsevier, Amsterdam 1989.

Golay, M.J. "Theory of Chromatography in Open and Coated Tubular Columns," in *Gas Chromatography*, D.H. Desty (Ed.), pp. 36–55 Academic Press, New York, 1958.

Kärger, J. and D.M. Ruthven, "Diffusion in Zeolites and other Microporous Solids," p. 299, John Wiley, New York, 1992.

Park, M., F.R. Rhodes, J.H. L'Amoreux, F.S. Baker, R.H. Beckler, and J.C. McCue, U.S. Patents 6,171,373, Jan. 9th 2001, and 6,284,705, Sept. 4th, 2001 to Westvaco Inc.

Ruthven, D.M., "Past Progress and Future Challenges in Adsorption Research," *Ind. Eng. Chem. Res.*, **39**, 2127–2131 (2000).

Ruthven, D.M. and S. Brandani, "Measurement of Diffusion in Porous Solids by Zero Length Column (ZLC) Methods" in *Recent Advances in Gas Separation by Microporous Ceramic Membranes*, N.K. Kanellopoulos (Ed.), pp. 187–212, Elsevier, Amsterdam, 2000.

Ruthven, D.M. and C. Thaeron, "Performance of a Parallel Passage Adsorbent Contactor," *Gas Sep. Purif.*, **10**, 63–73 (1996).

Spangler, G.E., "HETP Theory for Rectangular G.C. Columns," *Anal. Chem.*, **70**, 4805–4816 (1998).

Spangler, G.E. "Relationships for Modelling Performance of Rectangular Gas Chromatographic Columns," *J. Microcolumn Seps.*, **13**, 285–292 (2001).